

Self-avoiding walks and polygons on quasiperiodic tilings

A. N. Rogers¹⁾, C. Richard²⁾ and A. J. Guttmann¹⁾

¹⁾Department of Mathematics and Statistics
University of Melbourne, Victoria 3010, Australia

²⁾Institut für Mathematik, Universität Greifswald
Jahnstr. 15a, 17487 Greifswald, Germany

December 7, 2018

Abstract

We enumerate self-avoiding walks and polygons, counted by perimeter, on the quasiperiodic rhombic Penrose and Ammann-Beenker tilings, thereby considerably extending previous results. In contrast to similar problems on regular lattices, these numbers depend on the chosen initial vertex. We compare different ways of counting and demonstrate that suitable averaging improves convergence to the asymptotic regime. This leads to improved estimates for critical points and exponents, which support the conjecture that self-avoiding walks on quasiperiodic tilings belong to the same universality class as self-avoiding walks on the square lattice. For polygons, the obtained enumeration data does not allow us to draw decisive conclusions about the exponent.

1 Introduction

Quasiperiodic tilings are most widely used for the description of quasicrystals. With appropriate atomic decorations of the vertices, they serve as structure models which explain physical properties of quasicrystals [10]. From a theoretical point of view, they are idealisations of real substances on which the usual models of statistical physics like the Ising model may be studied [28, 29, 25]. Quasiperiodic tilings arose before the discovery of quasicrystals, however, more as an object of aesthetic interest in geometry [27, 20].

From a combinatorial point of view, they provide an interesting example of a non-periodic yet structured graph where typical problems of combinatorics like the counting of

objects on a lattice become more complex. This is fundamentally different from counting problems on semiregular lattices, where the underlying translational invariance is still present [17], and also from self-similar graphs, where the self-similarity allows for the solvability of some counting problems.

Consider for example the counting problem of n -step walks on a quasiperiodic tiling. This number depends on the chosen starting point. On a lattice, this phenomenon does not occur due to translation invariance. Questions arise, such as if the universal properties of the walks like critical exponents [26] are changed for quasiperiodic tilings¹, and how different ways of counting affect asymptotic properties. The first question has been investigated for self-avoiding walks (SAWs) and self-avoiding polygons (SAPs). These are walks or loops which do not visit the same vertex twice. Extrapolation of exact enumeration data for a number of quasiperiodic tilings [5, 28] indicates that the critical exponents γ for SAWs and α for SAPs are consistent with the corresponding values on regular lattices $\alpha = 1/2$ and $\gamma = 43/32$. In [22], the related problem of SAWs on Penrose random tilings [15] has been studied by Monte Carlo simulations, the results suggesting the same mean square displacement exponent as in the lattice situation. The studies [5, 28] suffered however from strong finite-size effects due to the relatively short series data available. This is mainly due to the fact that the finite-lattice method [9], being the most successful method known to date for walk enumeration on regular lattices [7, 8], cannot easily be applied here, and so we used the slower method of direct counting. The problem in applying the FLM is discussed in Section 3 below, see also [29]. Another reason for the pronounced finite-size behaviour is that the number of walks or loops depends on the chosen starting point. One might suspect that suitable averaging over different starting points reduces these effects, leading to behaviour comparable to the square lattice case. In this paper, we analyse three different methods of counting in detail. Whereas the first one depends on a chosen vertex of the tiling, the last two are averages over the whole tiling.

- *Fixed origin walks.* We count the number of n -step self-avoiding walks emanating from a given vertex. This number depends on the chosen vertex.
- *Mean number of walks.* We count all translationally inequivalent n -step self-avoiding walks which may occur anywhere in the infinite tiling, weighted by their occurrence probability. For tilings with quasicrystallographic k -fold symmetries, these probabilities are numbers in the underlying module $\mathbb{Z}[e^{2\pi i/k}]$. This leads to a generating function which has non-integer coefficients.
- *Total number of walks.* Here we count the number of translationally inequivalent n -step self-avoiding walks which may occur anywhere in the tiling. This number is bigger than the number of fixed origin walks, and by definition, takes into account vertices over the whole tiling.

Note that two self-avoiding walks (polygons) are translationally equivalent iff they have, up to a translation, the same vertex coordinates. For self-avoiding polygons, we will employ

¹For ferromagnetic spin systems on quasiperiodic graphs, a heuristic criterion determines whether its behaviour is different from the lattice situation [25].

the second and the third method of counting. We do not distinguish between different fillings of the interior of the polygon. For SAPs, the second method has been implemented previously [28] to obtain the high temperature expansion of the Ising model. The mean number of SAPs up to length $2n = 18$ has been determined on the Ammann-Beenker tiling [1, 18] and on the rhombic Penrose tiling [27, 6].

We counted SAWs and SAPs on the Ammann-Beenker tiling and the rhombic Penrose tiling and compared different counting schemes, thereby extending and generalising the previous approaches to counting SAWs [5] and SAPs [28]. Generally speaking, averaging reduces oscillation of data due to finite size effects, providing improved estimates for critical points and critical exponents. Within numerical accuracy, we cannot rule out the universality hypothesis that SAWs on the Ammann-Beenker and on the rhombic Penrose tilings have the same exponents as on the square lattice. The data for the total number of walks (polygons) gives a different exponent, reflecting the fact that the number of patches grows quadratically with the patch size, in contrast to the lattice case [21, 24]. The limited quantity of SAP data does not allow us to draw decisive conclusions about exponents.

This paper is organised as follows. The next chapters describe the algorithms used for the generation of the tilings and for the computation of the numbers of walks and their mean values. The following chapter is devoted to the asymptotic analysis of the series and to a comparison of the different approaches. This is concluded by a discussion of possible future work.

2 Graph generation

Quasiperiodic tilings in \mathbb{R}^d may be obtained by projecting certain subsets of lattices from a higher-dimensional space \mathbb{R}^n into \mathbb{R}^d . This is described by a *cut-and-project scheme*, summarised in the following diagram.

$$\begin{array}{ccccc}
 E_{\parallel} \simeq \mathbb{R}^d & \xleftarrow{\pi_{\parallel}} & E = \mathbb{R}^n & \xrightarrow{\pi_{\perp}} & E_{\perp} \simeq \mathbb{R}^m \\
 \cup & \nearrow_{1-1} & \cup & \nearrow_{\text{dense}} & \cup \\
 L_{\parallel} = \pi_{\parallel}(L) & & L \text{ lattice} & & W \text{ polytope}
 \end{array}$$

It consists of a Euclidean vector space E , together with orthogonal projections π_{\parallel} and π_{\perp} . The vector spaces $E_{\parallel} = \pi_{\parallel}(E)$ and $E_{\perp} = \pi_{\perp}(E)$ are called *direct* and *internal* space, respectively. Let $L \subset E$ be a lattice. The projections are such that $\pi_{\parallel}|_L$ is one-to-one and $\pi_{\perp}(L)$ is dense in E_{\perp} (or dense in some subspace of E_{\perp}). Let $W \subset E_{\perp}$ be a polytope (or a finite union of polytopes). The set W is also called the *acceptance window*. The set of tiling vertices $\Lambda(W)$ is defined by

$$\Lambda(W) = \{\mathbf{x}_{\parallel} \in L_{\parallel} \mid \mathbf{x} \in L \text{ and } \mathbf{x}_{\perp} \in W\}. \quad (1)$$

The edges of the tiling are defined by the following rule: The tiling vertices $\pi_{\parallel}(\mathbf{x})$ and $\pi_{\parallel}(\mathbf{y})$ are adjacent iff the lattice vectors \mathbf{x} and \mathbf{y} are adjacent.

For the Ammann-Beenker tiling [1, 18], we have $n = 4$ and $d = m = 2$. The lattice is $L = \mathbb{Z}^4$. The projections π_{\parallel} and π_{\perp} are defined as follows. For $\mathbf{x} \in \mathbb{R}^n$, we set

$$\begin{aligned}\mathbf{x}_{\parallel} &= \begin{pmatrix} 1 & \cos \frac{\pi}{4} & \cos \frac{2\pi}{4} & \cos \frac{3\pi}{4} \\ 0 & \sin \frac{\pi}{4} & \sin \frac{2\pi}{4} & \sin \frac{3\pi}{4} \end{pmatrix} \mathbf{x}, \\ \mathbf{x}_{\perp} &= \begin{pmatrix} 1 & \cos \frac{3\pi}{4} & \cos \frac{6\pi}{4} & \cos \frac{9\pi}{4} \\ 0 & \sin \frac{3\pi}{4} & \sin \frac{6\pi}{4} & \sin \frac{9\pi}{4} \end{pmatrix} \mathbf{x}.\end{aligned}\tag{2}$$

The acceptance window $W \subset \mathbb{R}^m$ is a regular octagon with unit side length centred at the origin, having edges perpendicular to the axes. A typical patch is shown in Figure 1.

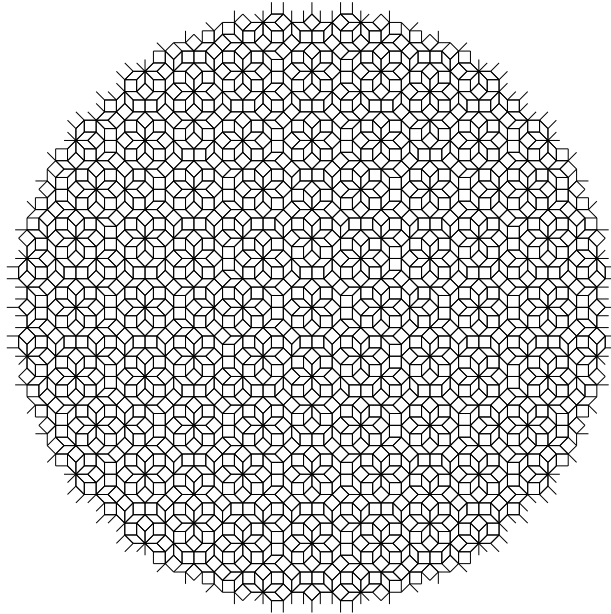


Figure 1: A patch of the Ammann-Beenker tiling.

For the rhombic Penrose tiling [27, 6], we have $n = 5$, $d = 2$ and $m = 4$. The lattice is $L = \mathbb{Z}^5$. The projections π_{\parallel} and π_{\perp} are, for $\mathbf{x} \in \mathbb{R}^n$, defined by

$$\begin{aligned}\mathbf{x}_{\parallel} &= \begin{pmatrix} 1 & \cos \frac{2\pi}{5} & \cos \frac{4\pi}{5} & \cos \frac{6\pi}{5} & \cos \frac{8\pi}{5} \\ 0 & \sin \frac{2\pi}{5} & \sin \frac{4\pi}{5} & \sin \frac{6\pi}{5} & \sin \frac{8\pi}{5} \end{pmatrix} \mathbf{x}, \\ \mathbf{x}_{\perp} &= \begin{pmatrix} 1 & \cos \frac{4\pi}{5} & \cos \frac{8\pi}{5} & \cos \frac{12\pi}{5} & \cos \frac{16\pi}{5} \\ 0 & \sin \frac{4\pi}{5} & \sin \frac{8\pi}{5} & \sin \frac{12\pi}{5} & \sin \frac{16\pi}{5} \\ 1 & 1 & 1 & 1 & 1 \end{pmatrix} \mathbf{x}.\end{aligned}\tag{3}$$

The acceptance window $W \subset \mathbb{R}^m$ is made up of four regular pentagons in the planes $\mathbf{x}_{\perp 3} = 0, 1, 2, 3$. The pentagons in the 0 and 3 x_3 -planes have unit side length and the others have side length $2 \cos \frac{\pi}{5}$. Each pentagon is centred at $\mathbf{x}_{\perp 1} = 0$, $\mathbf{x}_{\perp 2} = 0$. Pentagons 0 and 2 have an edge crossing the positive $\mathbf{x}_{\perp 1}$ axis at right angles while pentagons 1 and 3 are rotated through $\frac{\pi}{5}$. A typical patch is shown in Figure 2.

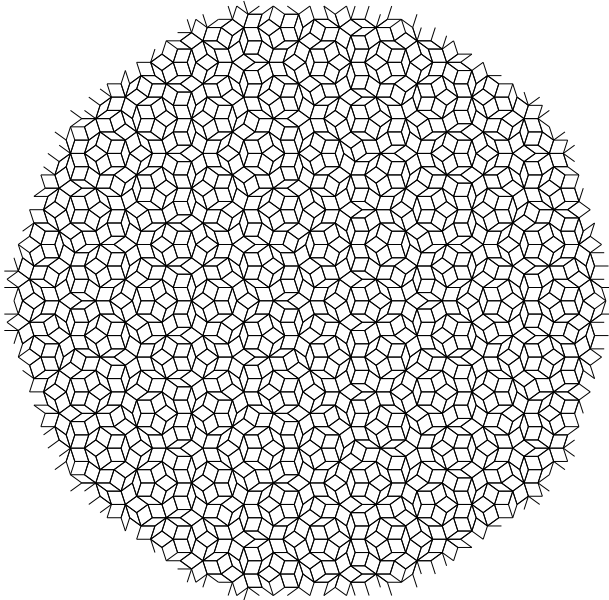


Figure 2: A patch of the rhombic Penrose tiling.

We remark in passing that a more natural embedding of the rhombic Penrose tiling is the root lattice A_4 , see also [3], but \mathbb{Z}^5 is more convenient for computations. Moreover, the Ammann-Beenker tiling and the rhombic Penrose tiling may be alternatively defined by inflation rules for their prototiles [4, 11].

3 Enumeration

A self-avoiding walk on a graph is a path, beginning at an origin vertex, which never visits a vertex more than once. The SAW on the lattice \mathbb{Z}^d is a well-studied object (see, for example, [26, 23]). The number c_n of translationally inequivalent n -step walks on a regular lattice is clearly independent of the choice of origin vertex. Hence this series is representative of the entire lattice. The enumeration of SAWs on non-periodic tilings introduces complications to the interpretation of the series $C(x) = \sum_{n \geq 0} c_n x^n$. This is because the possible origin vertices produce an infinite range of different series $C(x)$. Each origin produces a different series which is representative only of that vertex's immediate neighbourhood in the tiling. The question then is, how do we obtain a SAW series which is representative of the whole tiling? In this paper we adopt three different approaches to enumerating SAWs on quasiperiodic tilings, as described in the introduction. They are:

- *Fixed origin walks.*
- *Mean number of walks.*
- *Total number of walks.*

3.1 Fixed origin walks

We take a random selection of origin vertices $\mathbf{x} \in L$ (if $\mathbf{x}_\perp \notin W$ the vertex is not a suitable choice and is ignored). For each suitable origin, we generate the neighbourhood of the vertex, including all vertices up to some Euclidean distance N away. Two such neighbourhoods are shown in Figure 1 and Figure 2. We enumerate all SAWs from the origin up to length n in the neighbourhood using backtracking [31]. This takes time proportional to the number of walks c_n . Unfortunately, the transfer matrix approaches used to enumerate SAWs on regular two-dimensional lattices in less time cannot be used on this problem without major adaptation: Since a SAW of N steps may reach a vertex N steps from the origin, we would need to consider every possible tiling patch of radius N . The finite-lattice method's transfer matrix stage would then need to be adapted to each tiling patch, or generalised to handle them all.

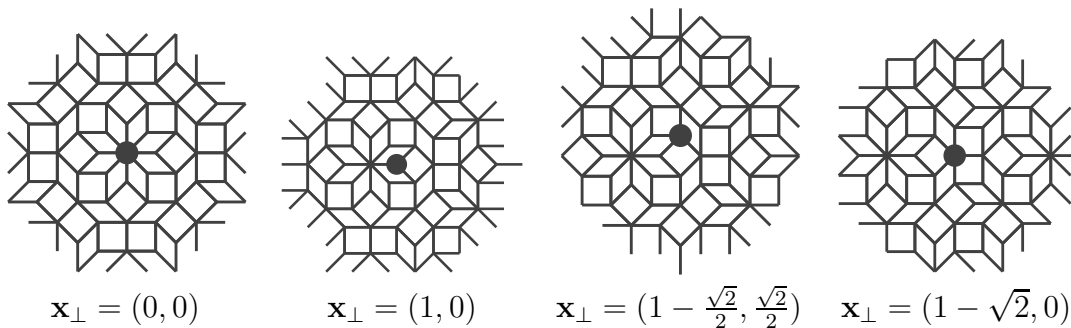


Figure 3: The actual Ammann-Beenker neighbourhoods chosen for the enumerations.

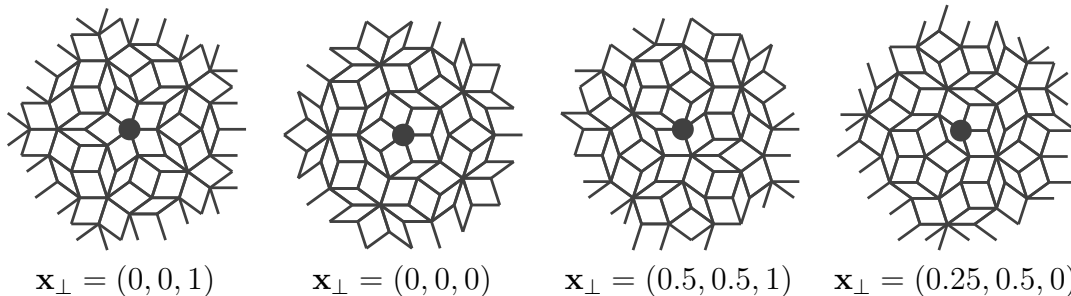


Figure 4: The actual rhombic Penrose neighbourhoods chosen for the enumerations.

If we apply this method to counting walks on a regular lattice it is clear that we would always produce the usual SAW series for that lattice. If each of the series in Table 1 and Table 2 showed lattice consistent properties, it would be a good indication that these properties belong to the entire tiling. The actual neighbourhoods chosen for the enumerations are shown in Figure 3 and Figure 4 for the Ammann-Beenker and Penrose tilings respectively.

n	$\mathbf{x}_\perp = (0, 0)$	$\mathbf{x}_\perp = (1, 0)$	$\mathbf{x}_\perp = (1 - \frac{\sqrt{2}}{2}, \frac{\sqrt{2}}{2})$	$\mathbf{x}_\perp = (1 - \sqrt{2}, 0)$
0	1	1	1	1
1	8	3	4	5
2	16	13	12	16
3	48	34	46	42
4	144	108	108	152
5	448	292	374	388
6	1088	952	976	1194
7	3680	2458	3042	3412
8	9584	7746	8330	9678
9	28336	21348	24556	27218
10	82960	61478	68376	79150
11	225408	177230	197820	217562
12	657536	495808	554108	628996
13	1834768	1412152	1576464	1741464
14	5140752	3985706	4400920	4968606
15	14584112	11125408	12531794	13724682
16	40222672	31617786	34541864	39209054
17	114683280	87149372	98846548	107503768
18	313146848	248799302	270221012	306845714
19	896810944	680172768	773046904	840463852
20	2437468000	1943692238	2109562128	2386875508
21	6958267152	5303535884	6011045200	6548653714
22	18981078176	15086983820	16431248782	18500898140
23	53728620912	41295324398	46538635588	50883461478
24	147472084608	116624466842	127704810544	142927122532
25	413887940176			

Table 1: The number of n -step fixed origin SAWs for various starting points \mathbf{x}_\perp in the Ammann-Beenker tiling, with starting point coordinates (x, y) given in the internal space.

n	$\mathbf{x}_\perp = (0, 0, 1)$	$\mathbf{x}_\perp = (0, 0, 0)$	$\mathbf{x}_\perp = (0.5, 0.5, 1)$	$\mathbf{x}_\perp = (0.25, 0.5, 0)$
0	1	1	1	1
1	5	5	5	4
2	20	10	14	12
3	40	40	50	46
4	160	130	130	112
5	450	310	406	394
6	1170	1140	1177	938
7	4000	2680	3316	3416
8	9480	9360	9723	7866
9	32910	23150	27356	27312
10	76090	72520	77747	66150
11	262250	196980	224102	215924
12	619460	555290	615549	545062
13	2050500	1646990	1812802	1698548
14	5052310	4292010	4869786	4411293
15	15828550	13403280	14455725	13367278
16	41103090	33637420	38524509	35243859
17	121759470	106779600	114089288	105117832
18	331072990	265198150	304434061	279216083
19	937563530	840669610	894584372	825140032
20	2642381430	2092703550	2399386239	2199738033
21	7227151280	6573888100	6988332717	6459329037
22	20931973090	16491425740	18844561759	17267339059
23	55793302330	51185968460	54473434666	50419312152
24	164764171030	129673789110	147471723662	135162732506

Table 2: The number of fixed origin n -step SAWs for various starting points \mathbf{x}_\perp in the rhombic Penrose tiling, with starting point coordinates (x, y, z) given in the internal space.

3.2 Mean number of walks

Given that a pair of vertices from $\Lambda(W)$ are adjacent if and only if they are adjacent in L , we see that the neighbours of a vertex with image \mathbf{x}_\perp can be found by sequentially adding the E_\perp image of all possible edges in L to \mathbf{x}_\perp and testing if the new points lie in W . If it does the adjacent vertex exists in $\Lambda(W)$. By recursively checking all possible neighbours of a vertex, all possible walks on the lattices will be found.

Given an origin vertex x^0 in $\Lambda(W)$, we know its E_\perp image x_\perp^0 must lie somewhere in W , i.e. $x_\perp^0 \in W^0 = W$ (W^n is the region x_\perp^0 can lie in given our knowledge of the n steps in the walk). If we take a step s (with projection s_\perp onto E_\perp) to a possible adjacent vertex x^1 , then we know $x_\perp^1 = x_\perp^0 + s_\perp$. Furthermore if $x^1 \in \Lambda(W)$ is true, $x_\perp^1 \in W$. Hence $W^1 = (W \cap (W^0 + s_\perp)) - s_\perp$. The probability that the step s is possible from a random x^0 is given by the ratio between the areas of W^1 and W .

Extending this to a walk of length n with steps $s^i, i = 1 \dots n$, $W^k = (W \cap (W^{k-1} + \sum_{i=1}^k s_\perp^i)) - \sum_{i=1}^k s_\perp^i$, the probability of the walk existing is the ratio of the areas of W^n and W . For example, consider the shaded W^i in Figure 5, for the particular walk in the Ammann-Beenker tiling which steps west, south, south-west, north-west, west, north then north. For the Ammann-Beenker tiling, these probabilities are of the form $a + b\lambda$, where $\lambda = 1 + \sqrt{2}$ and $a, b \in \mathbb{Q}$.

Adding the self-avoiding constraint and summing the probabilities results in the expected number of SAWs beginning at a random origin. Again note that applying this method to a regular lattice would result in the usual SAW series. Due to the extra complexity of the rhombic Penrose tiling acceptance window, the area calculations are more involved, see also [28]. They lead to mean numbers of the form $a + b\tau$, where $\tau = (1 + \sqrt{5})/2$ is the golden number, and $a, b \in \mathbb{Z}$. The rhombic Penrose tiling also allows steps in ten directions, more than the Ammann-Beenker tiling's eight. These facts combine to allow greater length series to be computed on the Ammann-Beenker tiling.

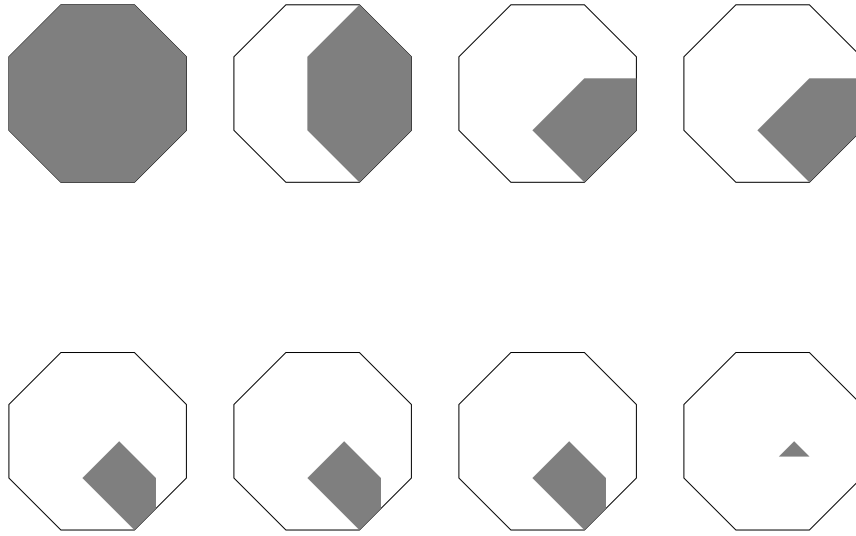


Figure 5: Examples of $W^0 \dots W^7$ for a particular walk on the Ammann-Beenker tiling.

n	Ammann-Beenker	rhombic Penrose
0	1	1
1	4	4
2	$52-16\lambda$	$62-30\tau$
3	$80-16\lambda$	$-4+28\tau$
4	$444-134\lambda$	$914-488\tau$
5	$1280-380\lambda$	$-820+732\tau$
6	$4492-1430\lambda$	$13842-7894\tau$
7	$10848-3248\lambda$	$-17732+12860\tau$
8	$60988-21700\lambda$	$173876-101988\tau$
9	$89800-27036\lambda$	$-255784+173720\tau$
10	$643248-237732\lambda$	$1923078-1143988\tau$
11	$979776-324200\lambda$	$-3149856+2073192\tau$
12	$5486960-2043420\lambda$	$19566548-11734706\tau$
13	$10785736-3819788\lambda$	$-34951044+22612992\tau$
14	$45253532-16927618\lambda$	$192557132-116151274\tau$
15	$110294592-40576780\lambda$	$-366912524+234803904\tau$
16	$375796808-141368464\lambda$	
17	$1058437232-398339560\lambda$	
18	$3259350860-1238175678\lambda$	
19	$9526156024-3632872284\lambda$	
20	$29127575440-11192322668\lambda$	
21	$81536068712-31337365980\lambda$	
22	$259724099656-100797073134\lambda$	

Table 3: The mean number of n -step SAWs for the Ammann-Beenker tiling and the rhombic Penrose tiling, where $\lambda = 1 + \sqrt{2}$ and $\tau = (1 + \sqrt{5})/2$.

3.3 Total number of walks

Investigating all possible walks as in the mean number of walks method, we count instead the number of non-zero contributions to the mean value. This counts the number of translationally inequivalent walks with W^n having positive area or, equivalently, the number of translationally inequivalent walks which may occur anywhere in the tiling. Again we note that applying this method to a regular lattice gives the usual SAW series.

n	Ammann-Beenker	Penrose
0	1	1
1	8	10
2	56	90
3	288	560
4	1280	2800
5	5344	12060
6	20288	48520
7	74192	182000
8	260336	658300
9	892800	2282400
10	2976512	7749440
11	9828256	25634920
12	31758112	83615140
13	101847216	268113660
14	322240144	850895040
15	1012048208	2668534600
16	3147031584	
17	9732815728	
18	29852932384	
19	91182029360	
20	276695822928	
21	836719766336	
22	2516664888416	

Table 4: The total number of n -step SAWs for the Ammann-Beenker tiling and the rhombic Penrose tiling.

3.4 Self-avoiding polygons

A self-avoiding polygon is equivalent to a self-avoiding walk in which the initial and final vertices are adjacent. In the enumeration of self-avoiding polygons, we do not distinguish between polygons having, up to a translation, the same boundary but different fillings of the interior.

SAPs may be enumerated in the same manner as we enumerate SAWs. The additional property of end point adjacency allows the backtracking algorithm to be pruned earlier. When enumerating SAPs up to size N , a walk that visits a vertex after D steps that is further than $N - D$ steps from the origin may be pruned from the search tree. Such a walk can never form part of a SAP of $\leq N$ steps. This was used to extend the length of the rhombic Penrose SAP series. The Ammann-Beenker SAP series were calculated at the same time as the SAW series and hence are of the same length. The extensive run time requirements precluded further series extension.

For the computation of occurrence probabilities of self-avoiding polygons, the loop vertices are taken into account, as described in Section 3.2 for the mean number of walks. If the self-avoiding polygon has n loop vertices $x^i \in \Lambda(W)$, where $i = 1, \dots, n$, the acceptance domain is $W^n = \bigcap_i (W - x^i_\perp)$, and the occurrence probability is given by the ratio between the areas of W^n and W , see also [28].

n	mean number	total number	mean number	total number
2	4	8	4	10
4	8	48	8	80
6	12λ	384	$108-48\tau$	840
8	$800-272\lambda$	2960	$240-64\tau$	6480
10	$2840-880\lambda$	21600	$6192-3364\tau$	49760
12	$28152-9984\lambda$	170256	$25584-13248\tau$	394080
14	$47712-9884\lambda$	1322048	$179200-95340\tau$	3087140
16	$869600-299392\lambda$	10194720	$162976-5440\tau$	24020160
18	$215712+294408\lambda$	79960896	$2704140-1067580\tau$	183529440
20	$14980920-3730840\lambda$	618248240		
22	$152588920-47048100\lambda$	4726263168		

Table 5: The mean number of n -step SAPs and the total number of SAPs for the Ammann-Beenker tiling (first two columns) and for the rhombic Penrose tiling (last two columns), where $\lambda = 1 + \sqrt{2}$ and $\tau = (1 + \sqrt{5})/2$.

4 Analysis of series

The various sequences were analysed using standard methods of asymptotic analysis of power series expansions as described in [12]. For self-avoiding walks and polygons, it is easy to prove that the limit $\lim_{n \rightarrow \infty} (c_n)^{1/n}$ exists by use of concatenation arguments [26]. We assume the usual asymptotic growth of the sequence coefficients c_n , viz:

$$c_n = Ax_c^{-n} n^{\gamma-1} [1 + \mathcal{O}(n^{-\epsilon})] \quad (n \rightarrow \infty, 0 < \epsilon \leq 1). \quad (4)$$

On the square lattice, there is overwhelming evidence [8] of the above asymptotic behaviour with $\gamma = 43/32$. There is however no proof of this assumption. For interesting new

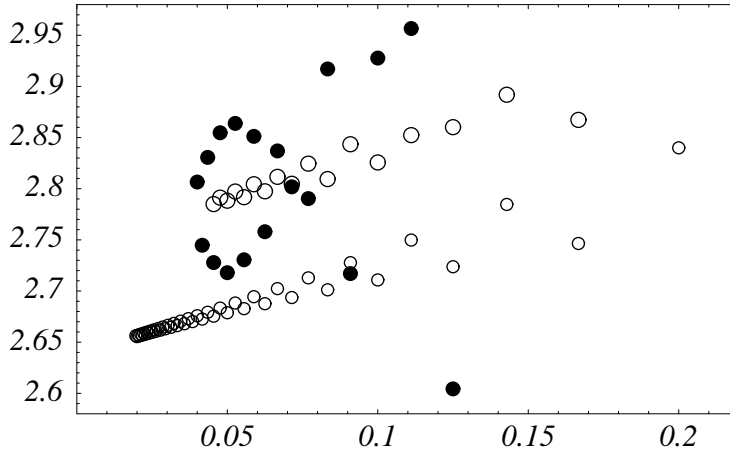


Figure 6: Ratio plot of c_n/c_{n-1} against $1/n$ for fixed origin (full circles) and mean number (large empty circles) Ammann-Beenker SAWs. The square lattice SAW data is plotted in small circles for comparison.

developments see [23]. The above assumption results in an asymptotic growth of the ratios r_n

$$r_n = \frac{c_n}{c_{n-1}} = \frac{1}{x_c} \left[1 + \frac{\gamma - 1}{n} + \mathcal{O}(n^{-1-\epsilon}) \right] \quad (n \rightarrow \infty, 0 < \epsilon \leq 1), \quad (5)$$

which may be used to extrapolate numerical estimates of x_c and γ . Whereas it has been proved for the square lattice that the limit $\lim_{n \rightarrow \infty} c_n/c_{n-2}$ exists and coincides with x_c^{-2} [19], a similar statement for the ratios r_n is not known. For some lattices, counterexamples are known [13].

Fig. 6 shows a plot of the ratios r_n against $1/n$ for a typical fixed origin Ammann-Beenker walk (full circles) and for the ratios of the mean numbers of Ammann-Beenker walks (large empty circles). We notice that the fixed origin data suffers from dramatic fluctuations, which are smoothed out by averaging, but are still larger than the corresponding square lattice data [8], which is shown in small circles. The oscillating behaviour of the mean number of walks data is due to an additional singularity of the sequence generating function at $x = -x_c$, which, for the case of the square lattice, is well understood due to anti-ferromagnetic ordering [8]. To obtain estimates of x_c and γ , we used the standard method described in [12] and first mapped away the singularity on the negative real axis by an Euler transform and then used Neville-Aitken series extrapolation.

We also used the method of differential approximants (DAs) [12]. The underlying idea is to fit a linear differential equation with polynomial coefficients to the generating function of the sequence, truncated at some order n_0 . The critical points and critical exponents of the differential equation are expected to approximate the critical behaviour of the underlying sequence. Application of first order and second order DAs has proved useful for the analysis of square lattice SAWs [12]. A first order DA involves fitting the coefficients to the differential equation $P_1(x)xf'(x) + P_0(x)f(x) = R(x)$ where $P_1(x)$, $P_0(x)$

and $R(x)$ are polynomials of degree N , M , and L respectively. We refer to this as a $[L/M; N]$ DA. We analysed the approximants $[L/N - 1; N]$, $[L/N; N]$, $[L/N + 1; N]$ for $1 \leq L \leq 8$. We computed estimates for x_c and γ by averaging of the different DA results, given a fixed number of series coefficients n_0 . Since this yields more accurate estimates of x_c and γ (typically of one digit better) than the ratio method and series extrapolation, we list in Table 6 only the results for the DA analysis. Note that the errors are no strict error bounds, but arise from averaging over approximants $[L/N_0; N_1]$ for different values of N_0, N_1 and L , as explained in [12].

	mean no.	(0, 0)	$(1 - \frac{\sqrt{2}}{2}, \frac{\sqrt{2}}{2})$	(1, 0)	$(1 - \sqrt{2}, 0)$
x_c	0.36414(18)	0.3659(14)	0.3644(13)	0.3644(21)	0.3657(16)
γ	1.325(19)	1.45(16)	1.30(14)	1.32(17)	1.46(17)

Table 6: Estimates of x_c and γ for Ammann-Beenker SAWs. Numbers in brackets denote the uncertainty in the last two digits.

As suggested by the ratio plot, the estimate using the data for the mean number of walks yields the most precise estimates, which are, however, one order of magnitude in error worse than the corresponding estimates for square lattice SAWs.

An analysis of the total number of SAWs on the Ammann-Beenker tiling using first order DAs yields $x_c = 0.3647(33)$ and $\gamma = 3.14(37)$. Whereas the critical point estimate is consistent with the previous analysis, the exponent estimate deviates from the value of $43/32 = 1.34375$ for fixed origin SAWs or the mean number of SAWs. This phenomenon reflects the fact that the number of Ammann-Beenker patches of radius r grows asymptotically as r^2 . (More generally, for aperiodic Delone sets in \mathbb{R}^d described by a primitive substitution matrix, the number $N(r)$ of patches of radius r grows like $N(r) \simeq r^d$ [24, 21].) Since the SAW has fractal dimension $4/3$, we expect an asymptotic increase of the number of SAWs by $n^{2\nu}$, where $\nu = 3/4$. Thus $\gamma = 43/32 + 2\nu = 2.84375$. Data extrapolation is consistent with this value.

The analysis of SAP data follows the same lines. However, the estimates suffer from large finite size errors due to the low number (11) of available coefficients. First order differential approximants for the mean number of SAPs yield $x_c = 0.3688(41)$. We assume $x_c(SAP) = x_c(SAW)$, which has been proven for the square lattice case [14].

For the critical exponent $\alpha = 2 + \gamma$, we expect for the mean number of SAPs by universality that $\alpha = 1/2$, being the believed exact value for the square lattice (and numerically confirmed to very high precision [16]). Due to lack of data it is not possible to give estimates of critical exponents. An analysis of the total number of SAPs on the Ammann-Beenker tiling using first order DAs yields $x_c = 0.3587(15)$.

The above analysis has also been applied to the rhombic Penrose tiling data. We observe qualitatively the same finite size behaviour as for the Ammann-Beenker tiling data, though the fluctuations are a bit less pronounced. In Table 7 we list estimates for x_c and γ obtained by analysing first order differential approximants.

An analysis of the total number of SAWs on the rhombic Penrose tiling using first

	mean no.	(0, 0, 0)	(0, 0, 1)	(0.25, 0.5, 0)	(0.5, 0.5, 1)
x_c	0.36322(29)	0.3621(12)	0.3613(16)	0.36248(83)	0.36347(51)
γ	1.333(26)	1.28(14)	1.19(22)	1.303(83)	1.387(62)

Table 7: Estimates of x_c and γ for Penrose SAWs. Numbers in brackets denote the uncertainty in the last two digits.

order DAs yields $x_c = 0.3638(31)$ and $\gamma = 2.77(21)$. The estimate of the critical point is consistent with the estimates from the other methods of counting. For the critical exponent, we again expect a value of $\gamma = 43/32 + 2\nu = 2.84375$, which agrees with the extrapolation within numerical accuracy.

For the analysis of SAP data, only 9 series coefficients are available. First order differential approximants for the mean number of SAPs yield $x_c = 0.372(11)$. An analysis of the total number of SAPs on the rhombic Penrose tiling using first order DAs yields $x_c = 0.3590(22)$. Again, due to lack of data, it is not possible to extrapolate reasonable estimates for the critical exponent α .

Conclusion

We extended previous enumerations for self-avoiding walks and polygons on the Ammann-Beenker tiling and on the rhombic Penrose tiling and extracted estimates for the critical point and critical exponent, using different counting schemes. It turned out that averaging with respect to the occurrence probability in the whole tiling leads to the best estimates, whereas data produced by fixing an origin leads to strong finite size oscillations. The results support the universality hypothesis that the critical exponents appear to be the same as for the square lattice, within confidence limits. For the total number of walks (polygons) we obtain a new exponent reflecting the polynomial complexity of the number of patches of the underlying tiling.

Since the results were obtained using the enumeration method of backtracking, one might ask if more efficient enumeration methods can be applied in order to substantially increase the length of the series, and hence the accuracy of the estimates. Unfortunately, the successful finite-lattice method cannot be applied in this case, without substantial development.

On a mathematically rigorous level, it may be possible to show the equality of the critical points for SAPs and SAWs on quasiperiodic tilings by appropriately modifying the existing proofs for the hypercubic lattice [14]. Furthermore, it would be interesting to carry out an analysis to determine if random walk behaviour can be proved for dimensions greater than four [26].

Self-avoiding polygons may also be counted by area. Since this leads to a three-variable generating function due to the different areas of the prototiles, it is tempting to ask whether the scaling behaviour of these objects is different from that recently found [30] for self-avoiding polygons on two-dimensional lattices.

Acknowledgements

The authors thank Michael Baake for bringing their attention to the above problem and Daniel Lenz for useful advice on substitution systems. CR would like to acknowledge funding by the German Research Council (DFG). AJG would like to acknowledge funding by the Australian Research Council (ARC).

References

- [1] Ammann R Grünbaum B and Shephard G C 92 Aperiodic tiles *Disc. Comp. Geom.* **8** 1-25
- [2] Baake M Grimm U Joseph D and Repetowicz P 2000 Averaged shelling for quasicrystals *Mat. Sci. Eng. A* **294-296** 441-445
- [3] Baake M Joseph D Kramer P Schlottmann M 1990 Root lattices and quasicrystals *J. Phys. A: Math. Gen.* **23** L1037-L1041
- [4] Baake M and Joseph D 1990 Ideal and defective vertex configurations in the planar octagonal quasilattice *Phys. Rev. B* **42** 8091
- [5] Briggs K 1993 Self-avoiding walks on quasilattices *Int. J. Mod. Phys. B* **7** 1569-1575
- [6] de Bruijn N G 1981 Algebraic theory of Penrose's non-periodic tilings of the plane *Indagationes Mathematicae (Proc. Kon. Ned. Akad. Wet. Ser. A)* **84** 39-52 and 53-66
- [7] Conway A R Enting I G and Guttmann A J 1993 Algebraic techniques for enumerating self-avoiding walks on the square lattice *J. Phys. A: Math. Gen* **26** 1519-34
- [8] Conway A R and Guttmann A J 1996 Square lattice self-avoiding walks and corrections to scaling *Phys. Rev. Letts.* **77** 5284-5287
- [9] Enting I G 1996 Series Expansions from the Finite Lattice Method *Nucl. Phys. B (Proc. Suppl)* **47** 180-7
- [10] Gähler F Kramer P Trebin H-R and Urban K 2000 *Proceedings of the 7th International Conference on Quasicrystals, Mat. Sci. Engin.* **294-296**
- [11] Grünbaum B and Shephard G C 1987 *Tilings and Patterns* (New York: Freeman)
- [12] Guttmann A J 1989 Asymptotic analysis of power-series expansions, in: *Phase Transitions and Critical Phenomena*, ed Domb C and Lebowitz J L (London: Academic) Vol. 13
- [13] Hammersley J M 1960 Limiting properties of numbers of self-avoiding walks *Phys. Rev.* **118** 656

- [14] Hammersley J M 1961 The number of polygons on a lattice *Math. Proc. Cambridge Phil. Soc.* **57** 516-523
- [15] Henley C L 1999 Random tiling models, in: *Quasicrystals: The State of the Art*, Eds. DiVincenzo D P and Steinhardt P J, Series on Directions in Condensed Matter Physics, vol 16, (Singapore: World Scientific) 2nd edition 459-560
- [16] Jensen I 2000 Size and area of square lattice polygons *J. Phys. A: Math. Gen.* **33** 3533-3543
- [17] Jensen I and Guttmann A J 1998 Self-avoiding walks, neighbour-avoiding walks and trails on semiregular lattices *J. Phys. A: Math. Gen.* **31** 8137-45
- [18] Katz A 1995 Matching rules and quasiperiodicity: The octagonal tiling, in: *Beyond Quasicrystals* ed Axel F and Gratias D (Berlin: Springer) 141-89
- [19] Kesten H 1963 On the number of self-avoiding walks *J. Math. Phys.* **4** 960-969
- [20] Kramer P and Neri R 1984 On periodic and non-periodic space-fillings of E^m obtained by projection *Acta Cryst. A* **40** 580-587 *Acta Cryst. A* **41** 619 (Erratum)
- [21] Lagarias J C and Pleasants P A B 2001 Local complexity of Delone sets and crystallinity *preprint math.MG/0105088*
- [22] Langie G and Iglói F 1992 Walks on the Penrose lattice *J. Phys. A: Math. Gen.* **25** L487-L491
- [23] Lawler G F Schramm O and Werner W 2002 On the scaling limit of planar self-avoiding walk *preprint math.PR/0204277*
- [24] Lenz D 2002 private communication
- [25] Luck J M 1993 A classification of critical phenomena on quasi-crystals and other aperiodic structures *Europhys. Lett.* **24** 359-364
- [26] Madras N and Slade G 1993 *The Self-Avoiding Walk* (Boston: Birkhäuser)
- [27] Penrose R 1974 The rôle of aesthetics in pure and applied mathematical research *Bull. Inst. Math. Appl. (Southend-on-Sea)* **10** 266-271
- [28] Repetowicz P Grimm U and Schreiber M 1999 High-temperature expansion for Ising models on quasiperiodic tilings *J. Phys. A: Math. Gen.* **32** 4397-4418
- [29] Repetowicz P 2002 Finite-lattice expansion for the Ising model on the Penrose tiling *J. Phys. A: Math. Gen.* **35** 7753-7772
- [30] Richard C Guttmann A J and Jensen I 2001 Scaling function and universal amplitude combinations for self-avoiding polygons *J. Phys. A: Math. Gen.* **34** L495-501
- [31] Sedgewick R 1992 *Algorithms in C++* 2nd ed (Reading: Addison-Wesley)